Journal of Ceramic Processing Research. Vol. 5, No. 2, pp. 106~113 (2004)

J O U R N A L O F
Ceramic Processing Research

Dielectric and impedance spectroscopic behaviour of alkali oxide - containing glass ceramics in the system $[SrO.TiO_2]$-$[SiO_2.B_2O_3]$

O.P. Thakur*, Devendra Kumar[a], Om Parkash[a] and Lakshman Pandey[b]

Solid State Physics Laboratory, Lucknow Rd., Delhi -110054 (India)

[a]Department of Ceramic Engineering, Institute of Technology, Banaras Hindu University, Varanasi - 221005 (India)

[b]Department of Post-graduate Studies and Research in Physics & Electronics, Rani Durgavati University, Jabalpur - 482001 (India)

Dielectric properties are strongly dependent on crystallization conditions, which determined the amount of $SrTiO_3$ and secondary crystalline phases and the microstructure of the glass ceramics. Earlier reports confirm that the crystallization of the $SrTiO_3$ phase in borosilicate (without an alkali oxide additive) as well as in aluminosilicate glassy matrix is found to be complex and difficult. Glass ceramics with varying amounts of alkali oxide (K_2O) have been prepared in the strontium titanate borosilicate glass system. The glasses were crystallized in the temperature range 1073-1325 K. It is observed that the pure strontium titanate ($SrTiO_3$) phase can be crystallized at higher temperature by choosing an optimum amount of alkali oxide (K_2O). Dielectric characteristics of glass ceramic samples were measured with respect to frequency (0.1 kHz to 1 MHz) and temperature (300 to 500 K). The value of the dielectric constant is higher when $Sr_2B_2O_5$ crystallizes as a primary phase while it decreases significantly when $SrTiO_3$ crystallizes as a major crystalline phase. The temperature coefficient of the dielectric constant (TCε) becomes negative as the $SrTiO_3$ phase crystallized out in the glass ceramics and the value of the dielectric constant increases with a higher crystallization temperature and time which finally decides the amount of the $SrTiO_3$ phase. Attempts have also been made to correlate the observed dielectric behavior with the electrical contribution of various crystalline phases, residual glassy matrix, crystal-glass interface region and electrode contribution using the impedance spectroscopic technique.

Key words: Borosilicate glass, Glass ceramics, Perovskite, Dielectric and impedance.

Introduction

Glass ceramics are polycrystalline materials produced by high-temperature, controlled nucleation and crystallization of glasses [1]. This is an efficient way of producing a uniform, pore-free and fine-grained microstructure, which is highly desirable in ferroelectric materials. The dielectric properties can be tailored for a particular application by choosing the proper ratio of glassy and crystalline phases in glass-ceramic specimens. Several workers have attempted to study the crystallization and dielectric behavior of perovskite glass ceramics such as $BaTiO_3$ [2-5], $PbTiO_3$ [6-9], $NaNbO_3$ [10, 11], $CaTiO_3$ [12], $LiTaO_3$ [13] and $Pb_5Ge_3O_7$ [14].

The dielectric properties of glass ceramics based on perovskite $SrTiO_3$ have also proven to be quite interesting due to the ambient temperature applications requiring temperature compensation of the dielectric constant. This is achieved by appropriate proportion between the negative temperature coefficient of $SrTiO_3$ and positive temperature coefficient of the residual glassy matrix [15]. Strontium titanate glass ceramics have a wide scope of applications such as, cryogenic capacitive temperature sensors [16, 17] and several other applications [18-20].

An investigation into the crystallization and dielectric properties of strontium titanate aluminosilicate glass ceramics was performed [21]. A similar study has also been made on the borosilicate glass system, but in both the systems, it was found that the crystallization of the $SrTiO_3$ phase is difficult [22]. Mostly, it results in the formation of $Sr_2B_2O_5$ and some other phases. However, it is found that the addition of Bi_2O_3 [23] and K_2O [24] in the borosilicate glass system results in the crystallization of the $SrTiO_3$ phase with a suitable amount of additive and proper heat treatment schedules.

It is the purpose of the present paper to report on the dielectric properties of various glass ceramic samples in the system $(SrO.TiO_2)$-$(SiO_2.B_2O_3)$ with K_2O additive, correlating the dielectric results with those of the crystallization study presented in the previous paper and the impedance of the glass ceramics. It was hoped that this investigation would lead to an increased understanding, facilitating future efforts at utilizing glass ceramics for dielectric applications.

*Corresponding author:
Tel : +91-11-23921692
Fax: +91-11-2313609
E-mail: omprakasht@hotmail.com

Experimental Procedure

Reagent grade raw materials of $SrCO_3$, TiO_2, SiO_2, H_3BO_3 and K_2CO_3 were mixed in proportionate amounts and melted in high grade alumina crucibles in the temperature range 1373-1623 K. The molten glass was quenched by pouring into cold rectangular aluminum mould and quickly pressed by another plate so as to have a uniform thickness of glass slabs. The glass obtained was then shifted to a preheated furnace in the temperature range 723-873 K for annealing. The amorphous state of the glasses was confirmed by X-ray diffraction. Differential thermal analysis (DTA) was carried out for the glass powder by DTA (Perkin-Elmer 700) with a heating rate of 10 Kminute^{-1}. Glass specimens were subjected to different heat treatment schedules as determined from the DTA analysis. The phase composition of crystallized specimens was examined by X-ray powder diffraction analysis using Cu-Kα radiation (Rich-Seifert Model ID 3000 diffractometer). Microstructures of polished and etched (etchant used was 5% HCl + 10% HF) samples were examined by SEM (Philips, Model PSEM 500)

Dielectric properties of different glass ceramic samples were measured with an Impedance Analyzer (HP 4192A LF) as a function of frequency (100 Hz-1 MHz) and temperature from room temperature to 250^{o}C. Temperature was stabilized within ±1^{o}C before each measurement. From the dielectric data of different glass ceramic samples measured at various temperatures, the complex immittance functions viz., impedance (Z*=Z'–jZ''), admittance (Y), permittivity (ε*) and dielectric modulus (M*=jwCoZ*) were determined. Impedance and modulus spectroscopic techniques were used to find out the equivalent circuit model that represents the electrical behavior of glass ceramic samples. Different resistive (R's) and capacitive (C's) components of the modeled equivalent circuit were determined by a 'complex non linear square (CNLS)' fitting program using 'IMPSPEC.BAS' software developed by Pandey [25].

Results and Discussion

Different parameters (glass transition and crystallization temperatures) obtained from DTA plots (Fig. 1) are given in Table 1. Strontium titanate borosilicate glass without alkali oxide addition (Glass A) depicts glass transition temperature (Tg) and single exothermic peak (crystallization peak, Tc) at about 700^{o}C and 916^{o}C respectively [22]. The addition of alkali oxide (K_2O) to the base glass (Glasses B, C and D) splits the exothermic peak into two or more and lowers the glass transition temperature. Resolution and widening between these exothermic peaks become quite pronounced at a higher concentration of alkali oxide in the base glass composition (Glass D). In the case of glass B, the first

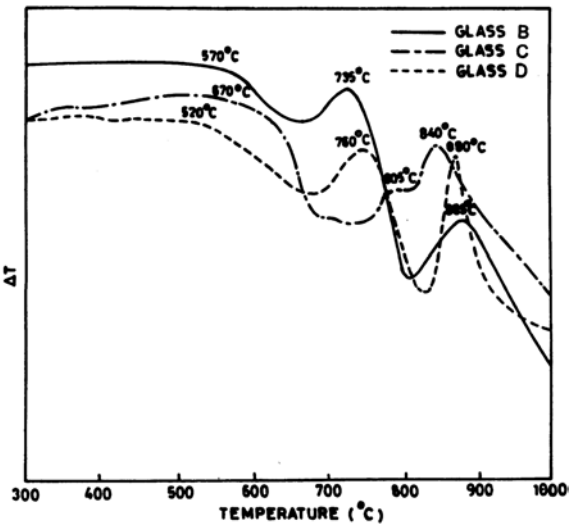

Fig. 1. DTA patterns of glasses B, C and D.

exothermic peak around 730^{o}C shows the formation of $Sr_2B_2O_5$ and $Sr_3Ti_2O_7$ phases while the second peak at 885^{o}C may be assigned to the precipitation of the TiO_2 (rutile) phase. From the various heat treatment schedules, it has been observed that at higher crystallization temperatures, the growth of the rutile phase (TiO_2) becomes quite fast. With increasing concentration of K_2O, the two exothermic peaks for the glass C come closer. The first peak shifts to a higher temperature (805^{o}C) while the second peak shifts to a lower temperature (840^{o}C). These crystallization peaks represent the formation of phases similar to glass B. In the case of glass D, these two crystallization peaks merge together and appear at 760^{o}C, which represents the crystallization of $Sr_2B_2O_5$, $Sr_3Ti_2O_7$ and TiO_2 phases. A new crystallization peak at 880^{o}C appears in this glass (glass D), which represents the formation of the $SrTiO_3$ phase. The crystallization of $SrTiO_3$ at higher temperature may be attributed to the re-dissolution of the rutile phase and the reaction of $Sr_2B_2O_5$ with TiO_2 (glass phase) [26].

A preliminary study of crystallization behavior and microstructural development of these glass ceramics was reported earlier [23]. The phase constitution of various glass ceramic samples, crystallized in the temperature range 900-1100^{o}C, is given in Table 2. In the strontium titanate borosilicate glass ceramic system, mostly $Sr_2B_2O_5$, TiO_2 (rutile) and $Sr_3Ti_2O_7$ phases

Table 1. Glass nomenclature and observed DTA peaks

Glass Name	Observed DTA peaks (^{o}C)			
	T_g	T_{c1}	T_{c2}	T_{c3}
A	700	–	916	–
B	670	735	885	–
C	670	805	840	–
D	680	–	760	880

Table 2. Heat treatment schedules, crystalline phases of different glass ceramic samples and temperature coefficient of dielectric constant (TCε) for some representative glass ceramic samples

Glass ceramic sample no.	Heat treatment schedules			Crystalline phases	TCε at 1 MHz (ppm K^{-1})
	Heating rate (K $minute^{-1}$)	Holding temp. (K)	Holding time (hrs)		
B1	5	900	3	SB+ST+R	+1761
B2	5	950	3	SB+ST+R	+1752
C1	5	800	3	R+SB+ST	–
C2	5	840	3	SB+ST+R	–
C3	5	900	3	SB+ST+R	+331
C4	5	950	3	SB+ST+R	+4238
D1	5	900	3	SB+ST+R	+1737
D2	5	950	0	P+R	–
D3	5	950	3	P+SB*+ST*	+1237
D4	5	950	12	P+R*	-105
D5	10	1050	3	P+R*	-344
D6	2	1050	10	P	-690
D7	0.5	1050	12	P	–

Note: * =trace amount, SB=$Sr_2B_2O_5$, ST=$Sr_3Ti_2O_7$, R=TiO_2 (rutile) and P=$SrTiO_3$ etc.

crystallized out during heat treatment in the temperature range 800-1000°C. There is a growth of $Sr_2B_2O_5$ crystallites from the central points forming "star like" patterns in these glass ceramics. Other phases like; $Sr_3Ti_2O_7$ and TiO_2 grow in between these large crystals [22]. An initial addition of K_2O promotes the formation of $Sr_2B_2O_5$ and $Sr_3Ti_2O_7$ and one obtains a similar microstructure to that of the base glass ceramics with a minor difference in grain size and their distribution. At higher K_2O concentration, phase separation occurs in glasses during the early stage of heat treatment. One region of the glassy phase may be rich in SrO and B_2O_3 while an other region is rich in TiO_2 and K_2O. At low heat treatment temperature, the $Sr_2B_2O_5$ phase crystallizes from the SrO and B_2O_3 -rich glassy region and small crystallites of TiO_2 form in the TiO_2 rich glassy region (glass ceramics sample D1). As the temperature is increased, $Sr_2B_2O_5$ crystallites react with components of the glasses and form $Sr_3Ti_2O_7$ and $SrTiO_3$ phases. At higher treatment temperatures (950-1100°C), $SrTiO_3$ remains as the major crystalline phase in glass ceramics (glass ceramic sample D3) and finally we get a glass ceramic product which contains only the $SrTiO_3$ crystalline phase (glass ceramic sample D4). With the addition of modifier (K_2O) to the borosilicate glass system, a lower temperature treatment gives $Sr_2B_2O_5$ and TiO_2 phases, which finally dissolved and gives $SrTiO_3$ phase at a higher crystallization temperature. This is due to the change in glass structure with the addition of the modifier alkali oxide [23]. A typical scanning electron micrograph of the glass ceramic sample D5 is given in Fig. 2. As is clear from this micrograph, sample D5 shows enhanced crystallization

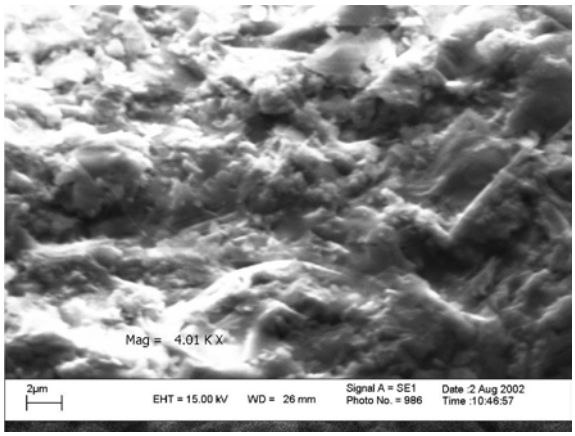

Fig. 2. Typical Scanning electron micrograph for glass ceramic sample D5.

of glass ceramics. The micrograph contains a few big crystals which grew with well defined angles and edges having an approximate size of 5 µm, and a very fine dispersion of $SrTiO_3$ crystals having a size less than 1 µm. The detailed microstructural study has been published elsewhere [23, 26].

Impedance and Dielectric Behavior

In the present glass ceramic system, complex modulus formalism (M*) is more suitable as it facilitates the construction of equivalent circuits and easy visualization of various charge transfer processes. Figures 3-5 illustrate the complex modulus plots at different temperatures for a few representative samples B2, C4 and D5 respectively. Two smeared and poorly resolved semicircular arcs on the higher frequency side reveal almost similar time constants whereas the third arc on the low frequency side shows relatively higher values of the time constant. It is to be noted that the data points on the locus of the modulus plots shift towards the lower frequency side as the temperature increases. Thus in complex plane modulus plots (M'' vs M') of different glass ceramic samples (Figs. 3-5), three arcs appear which show the presence of three parallel RC networks (R1C1, R2C2 and R3C3) connected in series with a blocking electrode capacitance (C4). Elements R1C1 (high frequency), R2C2 (mid frequency) and R3C3 (low frequency) have been assigned to crystalline phases, the glassy matrix and the crystal-glass interface region respectively. Approximate values of capacitance and resistance were determined from the intercept on the real axis and the maxima of semicircular arcs in the complex plane modulus plots respectively. The various R, C parameters determined by the complex non-linear square fitting (CNLS) program are listed in Table 3. R, C parameters calculated from the complex modulus and permittivity plots show consistency in results that verifies the proposed equivalent circuit. It is evident from Table-III that the values of resistance and capacitance

Table 3. Resistive and capacitive parameters of model equivalent circuit for different glass ceramic samples obtained by complex non linear square (CNLS) fitting

Parameters calculated	B1			B2			C4			D1			D3			D5		
	Temperature (K)			Temperature (K)			Temperature (K)			Temperature (K)			Temperature (K)			Temperature (K)		
	309	378	478	310	369	504	310	383	475	318	397	457	313	408	514	303	438	493
R1 (kΩ)	19.5	13.9	12.1	22	17.2	13.9	16.9	14.1	7.71	31.3	24.2	12	16.2	25	19.2	23.69	8.81	7.67
C1 (pF)	25.5	26.4	25.8	20.3	20.8	21	27.9	22.6	26.3	22.8	19.4	26	31.5	21.4	19	33.59	41.52	45.15
R2 (MΩ)	0.21	0.15	0.15	0.2	0.17	0.16	0.19	0.1	0.08	0.16	0.13	0.09	0.4	0.32	0.28	0.33	0.134	0.126
C2 (pF)	31.3	38	46	25	30	37.5	30.5	45	86	34.4	64	40.2	13	20	23.5	68.98	63.11	59.32
R3 (MΩ)	3.49	2.27	3.84	2.2	1.85	4.62	1.75	1.45	3.36	1.29	1.58	1.11	5	6	7	7.73	2.45	1.763
C3 (pF)	72.4	89	86	67	74	56	79	135	114	59	145	69	37	47	49	103	129	130
C4 (pF)	42	37	48	31.2	30	54.12	57.3	60	100	34	43	39	22	23	25	54.62	48.28	42.37
Γ1 (μS)	0.50	0.37	0.31	0.44	0.36	0.29	0.47	0.32	0.20	0.71	0.47	0.31	0.51	0.53	0.37	0.80	0.366	0.346
Γ2 (μS)	6.50	5.90	6.70	5.0	4.97	6.00	5.74	4.53	7	5.4	8.30	3.6	5.12	6.50	6.53	22.76	8.46	7.474
Γ3 (mS)	0.25	0.20	0.33	0.15	0.14	0.26	0.14	0.20	0.38	0.08	0.23	0.08	0.18	0.28	0.32	0.80	0.316	0.229

for the crystalline phase is smaller than that of the glassy and the crystal-glass interface region.

The dielectric behavior of this glass ceramic system shows a low value of dielectric constant and little temperature variation which can be understood as follows: crystallites (low value of resistance) in a glass ceramic specimen can be assumed to have impinged in the glassy matrix (relatively higher value of resistance). It is very clear from Table 3 that the magnitude of the crystal-glass interface resistance (R3) is significantly higher. As the AC signal is applied to the specimen, more charge gets transferred through the crystallites owing to their lower resistance, which gets stuck at the crystal-glass interface region (high resistance). On the other hand, a relatively small number of charges compared with the crystallites (R_{glass}>$R_{crystallites}$) travel through the glassy matrix and are impeded at the crystal-glass interface region. Consequently, the crystal-glass interface shows a high value of capacitance as compared to other components. A small temperature variation of capacitance (C1) for crystallites was observed which might be responsible for the temperature- independent behavior of the dielectric constant.

A complex plane modulus plots for the glass ceramic sample B2 is shown in Fig. 3. It is evident from this figure that at low temperature there is a poor resolution between the smeared semicircular arcs, which becomes quite distinct at higher temperature. Glass ceramic sample B2 shows a little higher resistance (R1) for the crystalline phase. This higher value of resistance may be due to enhanced crystallization of $Sr_2B_2O_5$, $Sr_3Ti_2O_7$ phases with a small amount of the TiO_2 (rutile) phase. The dielectric behavior for this glass ceramic sample B2 also shows a nearly temperature- independent behavior.

A complex plane modulus plots for glass ceramic sample C4 is shown in Fig. 4 at a few selected temperatures. The magnitude of the resistance of the crystalline phase (R1) for glass ceramic sample C4 is lower than

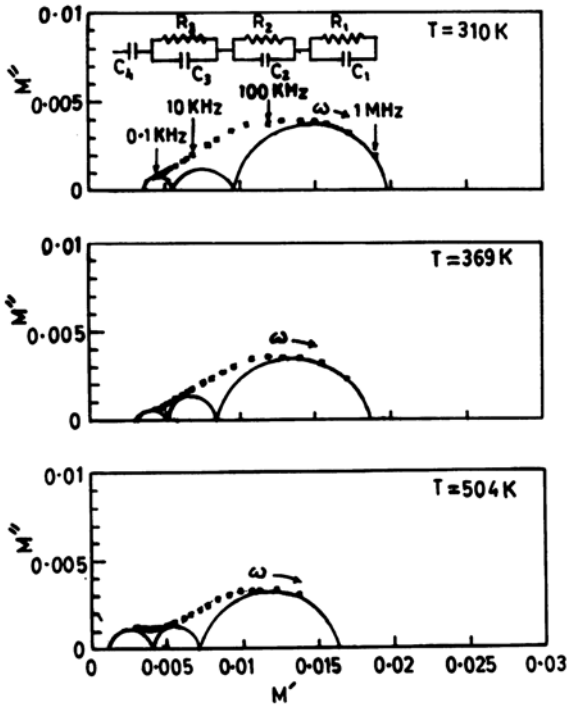

Fig. 3. Complex plane electric modulus plots for glass ceramic sample B2 at different temperatures.

that of B2 while the value of the capacitance (C1) is higher. The resistance (R1, R2) decreases with temperature for crystallites and the glassy matrix while it first decreases and then increases for the crystal-glass interface region (R3). The capacitance corresponding to the crystallites (C1) and the crystal-glass interface region (C3) shows an opposite trend, which in turn gives a diffuse maxima in the dielectric constant vs. temperature plots (Fig. 8).

From Table 3, we find that glass ceramic sample D1 shows a relatively higher value of resistance for the crystallites (R1) as compared to other glass ceramic samples while the resistance for the glassy matrix (R2)

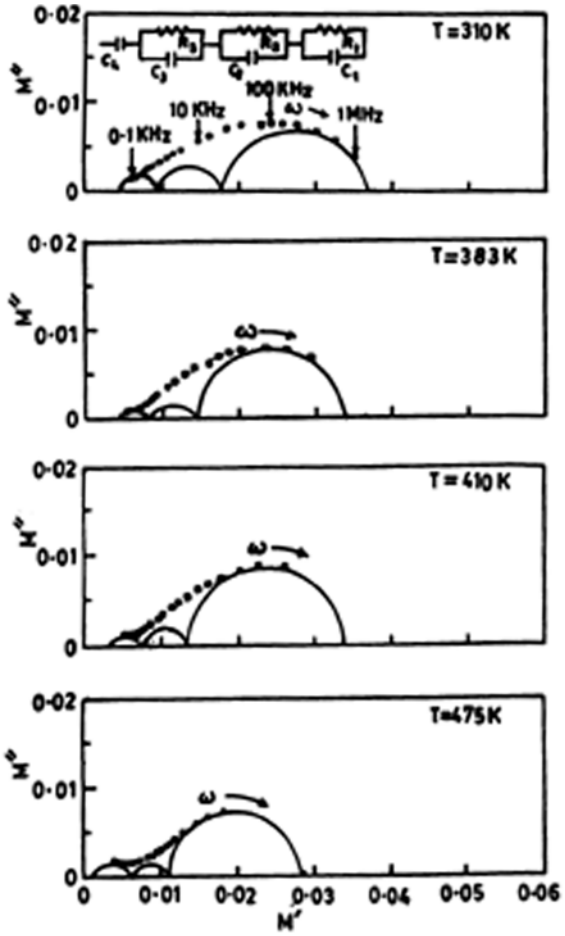

Fig. 4. Complex plane electric modulus plots for glass ceramic sample C4 at different temperatures.

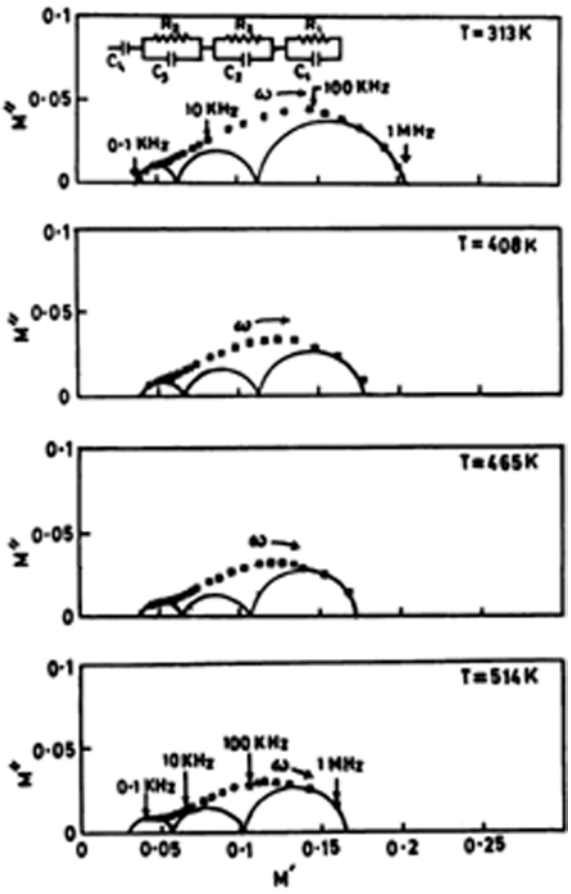

Fig. 5. Complex plane electric modulus plots for glass ceramic sample D3 at different temperatures.

and the crystal-glass interface region (R3) is relatively lower. Glass ceramic sample D3 shows the precipitation of the $SrTiO_3$ phase with traces of $Sr_2B_2O_5$ and $Sr_3Ti_2O_7$. Complex modulus plane plots as shown in Fig. 5 show relatively low values of capacitive blocking electrode contributions. For this sample (D3), the magnitude of the resistance corresponding to all the electroactive components is significantly higher as compared to other glass ceramic samples with different compositions and heat treatments while the capacitance shows opposite trend. This may be attributed to the more insulating nature of its electroactive components, very little charge is being accumulated at the crystal-glass interface region which results in a lower value of the dielectric constant for this glass ceramic specimen. The magnitude of the capacitance increases with temperature for the glass and the crystal-glass interface region while it decreases for the crystallites. This behavior is also confirmed from the earlier reports [16, 27] indicating a negative temperature coefficient of capacitance (TCC) of the $SrTiO_3$ crystalline phase and a positive temperature coefficient of the capacitance (TCC) for the glassy phase. It was also suggested that such a type of behavior can be exploited for ambient temperature applications requiring temperature compensation of the dielectric constant, which is achieved through the appropriate balance between the negative TCC of $SrTiO_3$ and the positive TCC of the glassy phase.

The representative dielectric behavior of the various glass ceramic samples at 405 K is shown in Fig. 6. The value of the dielectric constant decreases with increasing frequency and the dissipation factor shows a relaxation peak. The glass ceramic samples B2 and C4 containing $Sr_2B_2O_5$, $Sr_3Ti_2O_7$ and TiO_2 phases with a lower resistance show a strong dispersion in their dielectric behavior in comparison to glass ceramic sample D3 which contains the highly resistive $SrTiO_3$ phase. The observed dispersion is due to the relaxation of the space charge polarization across the glass-crystal interface region.

Glass ceramic sample B1 shows a dielectric constant and a dissipation factor in the range 30-40 and 0.01-0.15 respectively. The temperature dependence of the dielectric constant and the dissipation factor is small at the lower temperature, which becomes pronounced above 400 K. This may be attributed to increased interfacial polarization at the higher temperature. The temperature dependence of the dielectric constant and the dissipation factor for glass ceramic sample B2 is shown in Fig. 7 at different frequencies. Crystallization

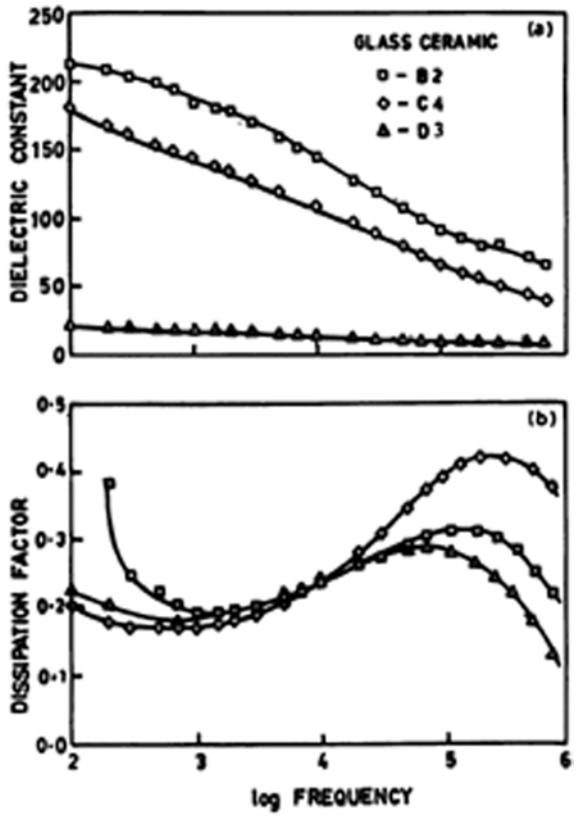

Fig. 6. Frequency dependence of (a) dielectric constant (ε') and (b) dissipation factor (tanδ) for glass ceramic sample B2, C4 and D3 at 405 K.

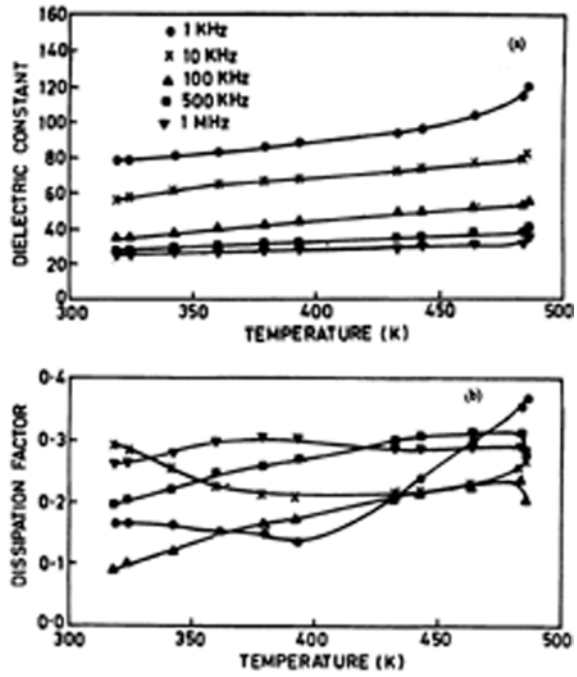

Fig. 7. Temperature dependence of (a) dielectric constant (ε') and (b) dissipation factor (tanδ) of glass ceramic sample B2 at different frequencies.

at higher temperature shows a relatively less temperature-dependent dielectric behavior. The magnitude of

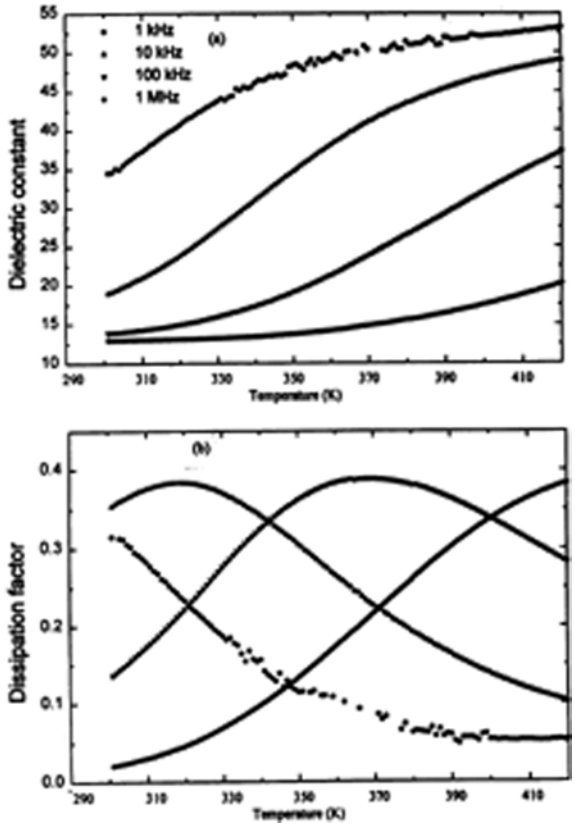

Fig. 8. Temperature dependence of (a) dielectric constant (ε') and (b) dissipation factor (tanδ) of glass ceramic sample C4 at different frequencies.

the dielectric constant and the dissipation factor falls in the range 20-120 and 0.1-0.3 respectively. An enhanced crystallization of of the resulting glass ceramics could be the reason for the higher value of the dielectric constant and the dissipation factor.

The dielectric behavior of glass ceramic sample C3 shows a temperature-independent behavior up to a certain temperature (400 K) and then levels off. The same trend was observed for the dissipation factor as well. The frequency dependence of the dielectric constant and the dissipation factor shows an appreciable dispersion in the low frequency region at higher temperatures. This phenomenon could be ascribed to space charge polarization. Figure 8 shows the temperature variation of the dielectric constant and the dissipation factor for glass ceramic sample C4. A large temperature variation is observed in the dielectric constant while the dissipation factor shows a maximum, which shifts towards higher temperatures with increasing frequency. This characteristic suggests that a thermally-activated process may be involved in the polarization of these glass ceramics.

The dielectric constant changes very little with respect to temperature for glass ceramic sample D1 (Fig. 9) and becomes temperature- independent at higher frequencies. The value of the dissipation factor decreases with temperature for the lower frequencies while it

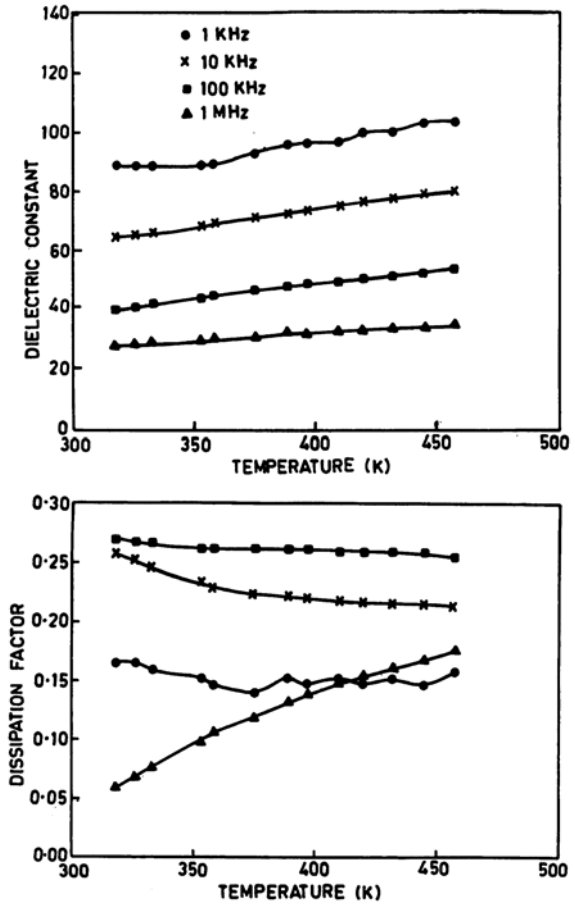

Fig. 9. Temperature dependence of (a) dielectric constant (ε') and (b) dissipation factor (tanδ) of glass ceramic sample D1 at different frequencies.

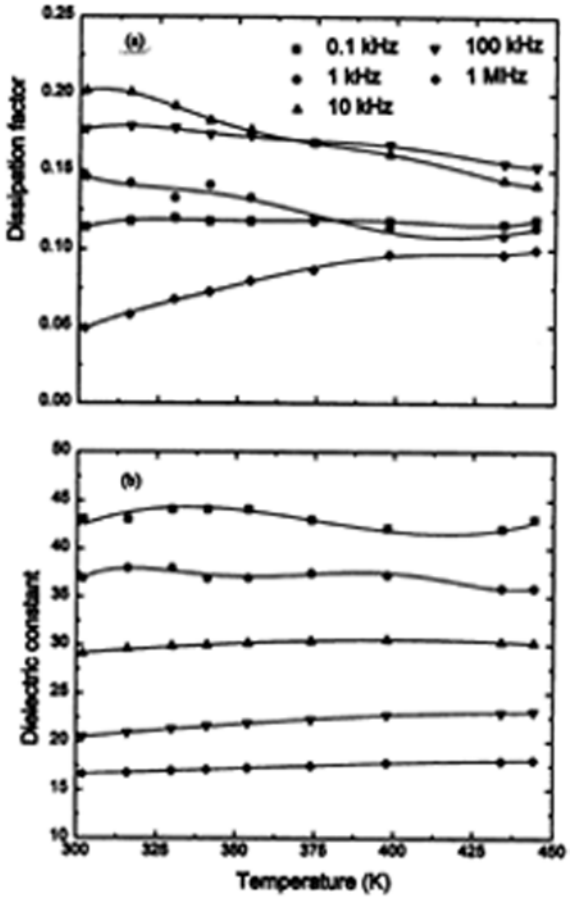

Fig. 10. Temperature dependence of (a) dielectric constant (ε') and (b) dissipation factor (tanδ) of glass ceramic sample D3 at different frequencies.

increases at higher frequencies. All these glass ceramic samples have similar crystalline phase constitution, containing $Sr_2B_2O_5$, $Sr_3Ti_2O_7$ and TiO_2 phases, and thus have similar dielectric behaviors. The difference in the values of the dielectric constant and the dissipation factor might be attributed to the differences in their microstructure. The temperature coefficient of the dielectric constant (TCε) for these glass ceramic samples is positive and listed in Table 2.

The temperature dependence of the dielectric constant and the dissipation factor for glass ceramic samples containing a major amount of the $SrTiO_3$ phase is shown in Figs. 10-11. Figure 10 illustrates the temperature dependence of the dielectric constant and the dissipation factor for glass ceramic sample D3 at different frequencies. Glass ceramic sample D3 contains perovskite $SrTiO_3$ as the major phase followed by the $Sr_2B_2O_5$ and $Sr_3Ti_2O_7$ phases. The value of the dielectric constant for this glass ceramic sample is approximately half that of the glass ceramic sample D1, in which strontium borate is the primary phase. The magnitude of the dielectric constant and the dissipation factor is 15-42 and 0.05-0.2 respectively. The temperature coefficient of the dielectric constant (TCε) is positive for glass ceramic sample D3, because at this crystallization temperature, a competition between $SrTiO_3$ and other crystalline phases ($Sr_2B_2O_5$, $Sr_3Ti_2O_7$) decreased the yield of $SrTiO_3$ in the glass ceramic, and the TCε became positive. Figure 11 shows the temperature variation of the dielectric constant for glass ceramic sample D4 in which a major amount of the $SrTiO_3$ phase is present. The magnitude of the dielectric constant lies in the range 20.5-23.5. The value of the

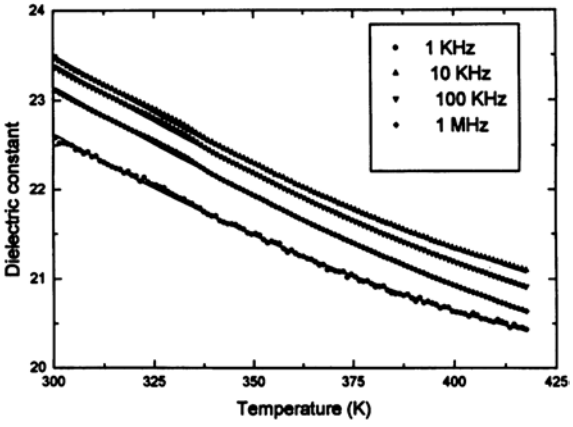

Fig. 11. Temperature dependence of dielectric constant (ε') of glass ceramic sample D4 at different frequencies.

dielectric constant decreases with an increase in temperature and a negative TCε (-105 ppm K^{-1}) is observed for this glass ceramic sample. There is no major change observed in the magnitude of the TCε with respect to frequency. The negative value of the TCε may be due to the crystallization of large amount of the $SrTiO_3$ phase [15]. This glass ceramic sample shows a very low value of the dissipation factor ($\leq 10^{-3}$). The same dielectric behavior was observed for glass ceramic sample D6 which also contains only $SrTiO_3$ as a crystalline phase in the resulting glass ceramics.

The value of TCε depends on the compensation between the negative temperature coefficient of $SrTiO_3$ and the positive temperature coefficient of the strontium titanate borosilicate glass which in turn depends on the amount of the glassy and $SrTiO_3$ phases.

For glass ceramic sample D3 in which the $SrTiO_3$ phase crystallized out along with $Sr_2B_2O_5$ and $Sr_3Ti_2O_7$ phases, the TCε is positive because the content of $SrTiO_3$ is relatively less as compared to the glassy matrix. The TCε of the glass ceramic samples becomes increasingly negative with increasing temperature and/or duration of the heat treatment. This is due to the increased amount of $SrTiO_3$ phase resulting in the glass ceramics. These observations are well supported from the Niesel's approximation model [28], which predicts that the dielectric constant would increase and the temperature coefficient of the dielectric constant (TCε) would decrease, becoming negative, as the volume fraction of $SrTiO_3$ was increased. This trend is identical to that observed with both the crystallization temperature and time in the present glass ceramics. Niesel's approximation has also been used earlier in studies of $BaTiO_3$ [29] and $PbTiO_3$ [30] glass ceramics.

Conclusions

(1) For lower concentration of K_2O, $Sr_2B_2O_5$ appears as the major phase followed by $Sr_3Ti_2O_7$ and TiO_2 phases similar to the base glass ceramic system. These show higher values of the dielectric constant.

(2) A higher K_2O concentration in the strontium titanate borosilicate glass system favors the crystallization of $SrTiO_3$ as a major phase with proper heat treatment schedules, which results in lower value of the dielectric constant and the dissipation factor. The value of the dielectric constant increases with the amount of the $SrTiO_3$ phase in these glass ceramics.

(3) The value of TCε becomes more negative as the content of the $SrTiO_3$ phase increases in the borosilicate glass ceramics.

(4) From impedance spectroscopy technique, it is evident that one can correlate the negative value of TCε with a decrease of capacitance corresponding to the presence of the crystalline phase with increasing temperature.

References

1. P.W. McMillan, in “Glass ceramics” (London: Academic Press, 1979).
2. O. Parkash, D. Kumar and R. Rajgopalan, Bull. Mater. Sci. 8 (1986) 13-21.
3. A. Herczog, J. Amer. Ceram. Soc. 47 (1964) 107-115.
4. D. Hulsenberg and J. Lehmann, Silikattechnik 34 (1983) 74-76.
5. A. Bhargava, R.L. Snyder and R.A. Condrate Sr., Mater. Lett. 7 (1988) 185-89 and 190-196.
6. T. Kokubo, H. Nagao and M. Tashiro, J. Ceram. Assoc. Jpn. 77 (1969) 293-297.
7. T. Kokubo and M. Tashiro, J. Non-Cryst Solids 13 (1973/1974) 328-334.
8. S. M. Lynch and J. E. Shelby, J. Am. Ceram. Soc. 67 (1984) 424-427.
9. J. Marrillet and D. Bourret, J. Non-Cryst. Solids 147 & 148 (1992) 266-270.
10. N.F. Borelli, J. Appl. Phys. 38 (1967) 4243-4247.
11. N.F. Borelli and M. M. Layton, J. Non-Cryst. Solids 6 (1971) 197-212.
12. T. Yamaguchi, H. Ayaki and L. Asai, J. Am. Ceram. Soc. 76 (1993) 993-997.
13. S. Ito, T. Kokubo and M. Tashiro, Bull. Inst. Chem. Res., Kyoto Univ. 54 (1976) 307-311.
14. S. Shimanuki, S. Hashimoto and K. Inomata, Ferroelectrics 51 (1983) 53-58.
15. S.L. Swartz, M. T. Lanagan, W.A. Schulze, L. E. Cross and W.N. Lawless, Ferroelectrics 50 (1983) 313-318.
16. W.N. Lawless, Cryog. Eng. 16 (1961) 261-264.
17. W.N. Lawless U.S. Patent No. 3 649891 (1972).
18. W.N. Lawless, Ferroelectrics 3 (1972) 287-293.
19. W.N. Lawless, J. Optic. Soc. Amer. 62 (1972) 1449-1454.
20. L.A.A. Warnes, Ultrasonics 29 (1991) 138-140.
21. S.L. Swartz, Ph.D. Thesis, Pennsylvania State University, University Park, PA, 1985.
22. O.P. Thakur, D. Kumar, O. Parkash and L. Pandey, Bull. Mater. Sci. 18 (1995) 577-585.
23. O.P. Thakur, D. Kumar, O. Parkash and L. Pandey, Indian J. Phys. 71A (1997) 161-167.
24 O.P. Thakur, D. Kumar, O. Parkash and L. Pandey, Materials Letters 23 (1995) 253-260.
25. L. Pandey, Workshop on use of computers in teaching physics, partly sponsored by ICTP, (Jabalpur, India), Dec 1992.
26. O.P. Thakur, Ph.D. Thesis, Banaras Hindu University, India (1998).
27. W.N. Lawless, Adv. Cryogenic Eng. 16 (1971) 261-267.
28. W. Niesel, Ann. Physik 6 (1952) 336-348.
29. S.L. Swartz, E. Breval, C. Randall and B.H. Fox, J. Mat. Sci. 23 (1988) 3997-4001.
30. D.G. Grossman and J.O. Isard, J. Mat. Sci. 4 (1969) 1059-1063.